MIT Open Access Articles

Optogenetic Stimulation of Lateral Orbitofronto-Striatal Pathway Suppresses Compulsive Behaviors

Massachusetts Institute of Technology

Optogenetic Stimulation of Lateral Orbitofronto-Striatal Pathway Suppresses Compulsive Behaviors

Eric Burguière[1], **Patrícia Monteiro**[1], **Guoping Feng**[1], and **Ann M. Graybiel**[*,1]

[1]McGovern Institute for Brain Research and Department of Brain and Cognitive Sciences, Massachusetts Institute of Technology, Cambridge, MA 02139 USA

Abstract

Dysfunctions in frontostriatal brain circuits have been implicated in neuropsychiatric disorders, including those characterized by the presence of repetitive behaviors. We developed an optogenetic approach to block repetitive, compulsive behavior in a mouse model in which deletion of the synaptic scaffolding gene, *Sapap3*, results in excessive grooming. With a delay-conditioning task, we identified in the mutants a selective deficit in behavioral response inhibition and found this to be associated with defective down-regulation of striatal projection neuron activity. Focused optogenetic stimulation of the lateral orbitofrontal cortex and its terminals in the striatum restored the behavioral response inhibition, restored the defective down-regulation, and compensated for impaired fast-spiking neuron striatal microcircuits. These findings raise promising potential for the design of targeted therapy for disorders involving excessive repetitive behavior.

Repetitive behaviors are cardinal features of a number of neuropsychiatric conditions (1, 2). Single behaviors and ritualistic sequences of behavior can be repeated compulsively to the point of seriously interfering with daily functioning (3). Attempts to find efficacious therapies for such conditions have been challenging (4, 5). Neuroimaging studies have identified abnormalities in cortico-basal ganglia circuits, particularly those involving the orbitofrontal cortex, implicated in the expression of repetitive, compulsive, and impulsive behaviors (6, 7). Disabling the lateral part of the orbitofrontal cortex (lOFC) reduces response inhibition and increases impulsive choice, and this deficit in response inhibition is likely related to abnormalities in orbitofrontal interactions with the striatum and associated basal ganglia circuits (7–10). We targeted this orbitofronto-striatal system to examine its function and to develop an optogenetic therapeutic approach to treat compulsive behavior. As a model, we focused on the compulsive behavioral responses exhibited by *Sapap3* mutant mice (11, 12), which exhibit spontaneous, repetitive facial over-grooming and anxiety, behaviors that could be considered analogous to pathological repetitive behaviors in obsessive-compulsive-disorder-spectrum disorders (13).

We first asked whether, as is thought to be the case in some human conditions, repetitive behavior in the *Sapap3* mutants could be triggered as an excessive reaction to a neutral stimulus that has been associated with a natural behavioral response. We designed a conditioning paradigm in which a neutral stimulus (a water drop applied to the forehead) provoked a grooming response that could be clearly identified, which allowed us to pair a tone with the water drop in a delay-conditioning paradigm (Fig. 1, A and B; fig. S1) (14).

The behavior of the *Sapap3* mutant mice and their wildtype littermates diverged sharply during the course of conditioning. Early on, both mutants ($n = 7$) and littermate controls ($n = 7$) readily became conditioned, grooming when the conditioning tone was played (Fig. 1, C and D). Later in training, the wildtypes began to inhibit this early grooming to the tone onset and to respond immediately after the water-drop release. The *Sapap3* mutants, by contrast, having once acquired the conditioned responses, kept responding to the tones with short-latency grooming, even in probe trials lacking water-drop delivery (Fig. 1, C to F, figs. S2 and S3, and table S1). This emergence of excessive short-latency responses was not accompanied by increased general grooming behavior or by hypersensitivity to the tone (figs. S4 and S5 and supplementary text). The *Sapap3* mutant mice thus expressed an acquired maladaptive behavior characterized by defective inhibition of their conditioned responses to the originally neutral tone stimuli.

Learning theories of human compulsive behavior suggest that repetitive behaviors can result from malfunction of a learning process that leads to loss of the ability to repress sensorimotor associations (3, 15, 16). To identify the neuronal basis of such a deficit, we recorded spike and local field potential (LFP) activity simultaneously with tetrodes in the lOFC and centromedial striatum as the mice acquired and then performed the task (fig. S6) (14). The baseline raw firing rates of putative pyramidal cells in the lOFC were similar in mutants ($n = 7$) and wildtypes ($n = 7$) throughout training, but the baseline firing rates of putative medium spiny neurons (MSNs) in the striatum were significantly elevated in the *Sapap3* mutants (Fig. 2, A and E).

During the early stages of training, sub-populations of pyramidal neurons in the lOFC in both genotypes exhibited a significant increase of activity between the tone and water events (Fig. 2B, fig. S7A, and table S2) (14). These lOFC responses remained similar throughout training; activity after the tone became progressively sustained up to the time of water-drop delivery (Fig. 2, B to D). By contrast, striatal task-related MSN activity patterns diverged markedly during training for the mutant and wildtype mice (Fig. 2, F to H; and fig. S7B) (14). Early on, MSNs in both genotypes exhibited a phasic increase in response to the tone; but the slope of this increase steadily declined in the wildtypes but did not in the *Sapap3* mutants (Fig. 2H). This tuning of MSN activity in the wildtypes occurred as their grooming onset times shifted toward the time of water-drop delivery (fig. S8).

The lack of such learning-related MSN tuning in the mutants could have reflected increased excitation or decreased inhibition of activity after the tone (see supplementary text). We considered one powerful source of MSN inhibition, deriving from fast-spiking striatal interneurons (FSIs), which mediate fast feed-forward inhibition of MSNs in response to cortical activation (17) and largely correspond to parvalbumin (PV)-containing interneurons. In cell counts of PV-immunostained sections, we found significantly fewer PV-positive striatal neurons in the mutants than in the wildtypes ($n = 8$ mice per genotype, chi-square test, $P < 0.05$) (fig. S9) (14).

This result suggested that a defect in intrastriatal inhibition could contribute to the *Sapap3* mutant phenotype but did not identify the source of the abnormality. In the light of clinical evidence (6, 9), we asked whether we could restore the striatal inhibition by optogenetically altering lOFC input to the striatum. We injected the lOFC bilaterally with adeno-associated virus (AAV5) to express a fusion protein of channelrhodopsin-2 and enhanced yellow fluorescent protein (ChR2-EYFP) under the calcium- and calmodulin-dependent protein kinase II (CaMKII) promoter (18) to target cortical pyramidal neurons of *Sapap3* mutant mice (fig. S10). We delivered pulses of blue light (473 nm, 5 mW, 10 Hz pulses) through two independently movable optical fibers and recorded neural activity simultaneously in the lOFC and striatum (Fig. 3, A and D, and fig. S11) (14). We confirmed expression of ChR2

and spike and LFP modulation at the stimulation frequency (Fig. 3, B and C, and figs. S10 and S11). Control experiments with non-effective laser stimulation and with control virus were negative (fig. S12).

We stimulated the ChR2-containing lOFC axon terminals within the striatum while we recorded from ensembles of striatal neurons (Fig. 3D). To assess specifically the direct effect of lOFC stimulation on FSIs and MSNs in the *Sapap3* mutants, we isolated 10 FSI-MSN pairs in which both members of the pair were recorded on the same tetrode (Fig. 3E and figs. S7B and S13) (14). In these recordings, MSN spiking was inhibited after FSI spikes, and this inhibition was greatly increased during optogenetic stimulation of lOFC terminals in the striatum (unpaired *t* test, $P < 0.01$). This effect could also be seen at the population level (Fig. 3, F and G). These dynamics suggest that activation of the lOFC-striatal pathway in the *Sapap3* mutants compensated for their abnormally high MSN activity at the end of the training by eliciting a powerful feed-forward inhibition of MSNs driven by the cortical activation of FSIs (19).

We applied this lOFC-striatal optogenetic stimulation at the end of training and showed that it could restore MSN tone-response inhibition in the *Sapap3* mutants (Fig. 3H). We then asked whether such stimulation could also ameliorate the behavior of the *Sapap3* mutant mice (Fig. 4, A to D). At the end of the training, we excited either projection neurons in the lOFC or their terminals in the striatum in different experiments, triggering the laser at tone onset and continuing it for 2.5 s at 10 Hz. When the *Sapap3* mutants were under optical stimulation, their early grooming responses to the tones were almost completely abolished, both by lOFC stimulation ($n = 4$) (Fig. 4, A, B and E) and by striatal stimulation ($n = 3$) (Fig. 4, C to E). Yet the mutants groomed normally as soon as the water drop was delivered. The abnormal stimulus-evoked compulsive behavior in the *Sapap3* mutants thus could have resulted from a deficit of behavioral inhibition that was restored by optogenetically stimulating the lOFC-striatal pathway.

We next tested whether we could also rescue the spontaneous compulsive phenotype of the *Sapap3* mutants by optogenetically stimulating in lOFC ($n = 6$) or striatum ($n = 4$) during their unconditioned, natural behavior, which is typified by excessive grooming, but for which the triggers impelling the grooming behavior are unknown (Fig. 4F) (14). Stimulation (5 Hz, 5 mW, 5-ms pulse for 3 min) almost fully alleviated their compulsive grooming (Fig. 4F), leaving intact other out-of-task behaviors requiring fine motor coordination and motivation ($n = 5$) (Fig. 4G). Wildtypes expressing CaMKII-ChR2 ($n = 3$) and *Sapap3* mutants expressing control virus ($n = 3$) showed no difference in grooming with the laser on and off (Fig. 4F).

Our findings demonstrate that selective stimulation of the lOFC-striatal pathway can restore a behavioral inhibition signal in an animal model expressing pathological repetitive behaviors and can prevent over-expression of both conditioned and spontaneous repetitive grooming. Optogenetic stimulation increased inhibition of striatal MSNs in the mutants, and it specifically activated striatal FSIs and affected FSI-MSN striatal microcircuitry. The abnormally elevated MSN baseline firing rates in the *Sapap3* mutant striatum and reduced numbers of PV-immunostained striatal interneurons, likely corresponding to physiologically identified FSIs, suggest that the microcircuit necessary for inhibiting MSN responses through FSI excitation may not have been fully functional (supplementary text) (11, 13).

A pathologic decrease of PV-containing striatal neurons has been observed in Tourette's syndrome, and FSI microcircuits have been implicated in other extrapyramidal disorders (20, 21). Our findings suggest that a key role of the lOFC in underpinning response

inhibition could include specific effects on FSI-MSN microcircuitry by which the lOFC controls striatal neurons (supplementary text).

Our finding that optogenetic control of this lOFC-striatal pathway can alleviate repetitive behaviors in a genetic model of compulsive behavior raises important questions for future work (supplementary text). Are sub-systems of striatal MSNs (e.g., D1 and D2 dopamine receptor-expressing neurons or striosome and matrix neurons) differentially affected (22–25)? Can this targeted optogenetic therapy alleviate repetitive behaviors in other models? What microcircuits underlie the normal orbitofronto-striatal pathway neuroplasticity and behavioral adaptation evident in the wildtypes? Our findings should provide a platform for exploring these differential influences and for developing new potential therapeutic targets to alleviate conditions characterized by abnormally repetitive behavior.

Materials and Methods

Animals

Forty-two mice (24 *Sapap3* mutants and 18 wildtype littermates, male, 3–l9 months old, C57BL6/J background) were maintained under a 12 h light/dark cycle with ad libitum food and water. Each *Sapap3* mouse in the grooming conditioning task was intentionally chosen as not having a facial skin lesion prior to the experiment (despite having excessive grooming behavior) so that lesion-induced skin sensitivity would not be a confounding variable influencing reactions to water drops.

Tetrodes, optical fibers and headstage

Custom-built headstages with 8 independently mobile microdrives weighed ~3 g and were made of plastic and brass (26). Microdrives were designed to hold either a tetrode (twisted 12-μm Ni/Cr wires) or an optical fiber (100 μm diameter) inserted in a zirconia ferrule. A spout was fixed at the front of the headstage to permit delivery of water drops onto the animal's forehead.

Surgical procedures

Each mouse was deeply anesthetized (1–2% isoflurane) and was mounted in a stereotaxic frame with non-puncturing ear bars. Small openings (2 mm wide) were made over the left central caudoputamen (AP = +0.2 mm, ML = +1.5 mm) and lateral orbitofrontal cortex (AP = +2.8 mm, ML = +1.5 mm), and AAV virus (0.2 μl) was injected with graduated pipettes at a rate of 0.02 μl/min. Several small burr holes (0.6 mm) were drilled around the perimeter of the exposed skull surface to accept brass anchor screws. The headstage was then fixed to the skull and screws with dental acrylic. Tetrodes were advanced individually over 5–7 post-operative days and were carefully put into position in the striatum (DV = 2.2–2.8 mm) and orbitofrontal cortex (DV = 1.5–2 mm), with an attempt to maximize the number of recorded units per site prior to the first training session. The tetrodes then were left in place throughout training, except for rare small adjustments (movements of less than 25 μm) to maintain multiple-unit recording at the same location over training. Throughout the entire training, we moved 7 of the 98 total tetrodes, each by an estimated distance of 25–50 μm.

Opsin delivery and optical stimulation in neural tissue

The adeno-associated viruses AAV-CaMKIIa-ChR2-EYFP and AAV-CaMKIIa-EYFP were packaged as AAV5 by the University of North Carolina vector core facility. These viral vectors have been shown to be expressed selectively in excitatory neurons (but not in neurons expressing GABA) when injected into the neocortex, with a level of transduction efficacy and expression of ChR2 of about 90% (27, 28). In all experiments, a minimum of 4

weeks elapsed before optical stimulation. Chronic optical fiber implants (Doric) were connected to optical patch cables coupled to 473-nm laser equipped with a collimator. Optical stimulation was controlled by a stimulus pulse generator and by signal pulses generated by digital input/output board.

The grooming conditioning task

Mice were allowed to recover for at least 7 days after surgery before any behavioral experimentation. The conditioning task was performed in a rectangular enclosure (15×25×15 cm) composed of anti-static plastic walls and a transparent Plexiglas floor (Fig. 1A). Mice were first habituated to the experimental box for several days. Each daily conditioning session consisted of 40 paired trials and 10 probe trials. In the paired trial, an 8 kHz tone was presented 1.3 s before the delivery of a water drop to the forehead of the mouse through the spout connected to a computer-controlled pump (Fig. 1B). The tone terminated simultaneously with the water drop. In the 10 probe trials randomly inserted within the 40 paired trials, the 8 kHz tone sounded for 1.3 s without water-drop delivery. Mice were allowed to groom freely in response to the tone and water. The inter-trial intervals began when the mice stopped grooming and were randomized in length (30–60 s). Each training session was conducted in dim light and lasted approximately 1 h. Grooming behavior was recorded with a video camera placed under the experimental box. Grooming onset events were assigned at the time when the mouse' front paws reached its nose to engage in phase 1 of grooming as defined in (29, 30). At the end of the training lasting at least 16 consecutive days, a subset of the *Sapap3* mutant mice ($n = 7$) were exposed to an extra session with laser stimulation delivered from 0.2 s before to 2.5 s after the tone onset (5 mW, 5-ms pulses, 10 Hz).

Out-of-task optogenetic stimulation

We delivered steady optical stimulation (5 mW, 5-ms pulses, 5 Hz) to mice placed in the experimental box without applying the conditioning protocol. Three-minute periods with and without continuous light stimulation were alternated consecutively 5 times.

Free-feeding behavioral task

Mice were food deprived for 3 days prior to this control experiment. The durations of feeding and food consumption were measured for each 5-min period with or without light stimulation. The light on/off periods were alternated twice for a 20-min total duration.

Data acquisition and analysis

Stimulus events (tone onset, water drop delivery, laser stimulation) were recorded during all training sessions, along with behavior (video) and neuronal activity. Neuronal recording of MSN and FSI activity with laser stimulation were performed after the training. Unit activity (gain: 200–10,000, filter: 600–6,000 Hz) was recorded with a Data Acquisition System. Spikes exceeding a preset voltage threshold were sampled at 32 kHz and were stored with time-stamps. For local field potential recording, neural signals were amplified (gain: 1,000), filtered (1–475 Hz) and sampled at 1 kHz. The spectral content of the local field potential signals was analyzed using open-source Chronux algorithms (http://chronux.org), in-house software, and the Matlab Signal Processing Toolkit. Spectrograms were constructed by the multitaper method, with three tapers, time bandwidth product of 2, and window width of 0.75 s.

Unit activity containing spikes of multiple neurons was sorted manually off-line into putative single units according to multiple spike parameters (e.g., peak height, valley depth, peak time) on the 4 channels of each tetrode. The accuracy of spike-sorting and the quality

of the single units were then evaluated by the use of spike waveform overlays to confirm uniform waveforms for a given unit and autocorrelograms to detect the presence of an absolute refractory period. Based on these tests"clusters" judged as being noise were excluded from the analysis. We classified as putative excitatory pyramidal cells neurons in which the baseline firing rate averaged over 50 trials did not exceed 10 Hz, with a spike width (at half-peak amplitude) within a range of 110–220 μs. With this criterion, we selected 79.1% (480/607) of the total units recorded in the lOFC (fig. S7A). For the striatal units, a unit with the average baseline firing rate of 5 Hz or below and with a spike width (at half-peak amplitude) within a range of 130–250 μs was classified as a putative MSN (fig. S7B). With this criterion, we identified 81.5% (495/608) of the units recorded in the striatum as putative MSNs. We classified as putative FSIs recorded units with the average baseline firing rate exceeding 10 Hz and with a spike width within a range of 70–120 μs (fig. S7B). We identified 4.3% (26/608) of the striatal units as putative FSIs. Units that did not meet these criteria (putative tonically active neurons, other types or noisy units) were excluded from the analysis. A unit (either putative MSN or putative pyramidal neuron) was further classified as ''task-related" unit if its firing rate between the tone and water-drop events was greater than 2 standard deviations above its pretrial baseline firing rate (2 s before the tone event) for at least three consecutive 50 ms bins.

For statistical analyses, statistical significance was assessed using repeated measures analysis of variance (ANOVA) on the entire training period, unpaired t-tests (with Bonferroni correction in case of multiple comparisons) and chi-square tests. Data were analyzed using Statview and SPSS software.

Histology

At the end of training, mice were deeply anesthetized (Nembutal, 50–100 mg/kg), and lesions were made to mark the final recording sites (25 μA, 10 s). Mice were then perfused with 4% paraformaldehyde (PFA) in 0.1 M sodium-potassium phosphate buffered saline (PBS), and 30 μm thick transverse frozen sections were stained for Nissl substance to identify lesion sites and by immunohistochemistry for GFP protein to confirm viral expression.

Immunostaining and cell count

Eight *Sapap3* mutant mice and eight age-matched wildtype mice (3–10 months) were compared for this study. Mice were anesthetized by isoflurane inhalation and transcardially perfused with cold PBS solution followed by 4% PFA fixative solution. Brains were coded in order to blind the experimenter of the mice genotype and were kept in 4% PFA overnight at 4°C. Brains were then transferred to PBS and sectioned at 50μm on a Vibratome. Two to six matched coronal sections (every 50 μm from 0.05–0.30 mm relative to Bregma point) containing the striatum from each animal were selected according to the mouse brain atlas. Sections were washed 3 times in PBS and incubated in 1.2% Triton-X 100 for 15 min, followed by another PBS wash (3 times). Blocking was performed for 1 h in PBS containing 2% BSA and 0.2% Triton-X. Mouse anti-parvalbumin antibody (Swant, PV235, 1:5000) was incubated overnight at 4°C. Next day, sections were washed 3 times in PBS, followed by 2-h room temperature incubation in biotinylated goat anti-mouse antibody (Jackson ImmunoResearch, 115-065-003). Sections were then washed and processed using the Vectastain ABC kit (Vector Laboratories, PK-4000) and DAB substrate kit for peroxidase (Vector Laboratories, SK-4100). Sections were mounted in Krystalon and imaged at the highest focal plane (to control for potential differences in labeling due to focal depth changes) using a microscope, 20X objective. Cells were counted from a 500×500 μm region defined according to the area of recording for both hemispheres in each section (fig. S6B;

ML: 1.0–1.5 mm, DV: 2.0–2.5 mm). Statistical analysis was performed using a chi-square test on the total number of cells counted in both genotypes.

Supplementary Material

Refer to Web version on PubMed Central for supplementary material.

Acknowledgments

References and Notes

1. Leckman JF. Tourette's syndrome. Lancet. 2002; 360:1577. [PubMed: 12443611]

2. Ridley RM. The psychology of perserverative and stereotyped behaviour. Prog. Neurobiol. 1994; 44:221. [PubMed: 7831478]

3. Franklin ME, Foa EB. Treatment of obsessive compulsive disorder. Annu. Rev. Clin. Psychol. 2011; 7:229. [PubMed: 21443448]

4. Otte C. Cognitive behavioral therapy in anxiety disorders: Current state of the evidence. Dialogues Clin. Neurosci. 2011; 13:413. [PubMed: 22275847]

5. Goodman WK, Lydiard RB. Recognition and treatment of obsessive-compulsive disorder. J. Clin. Psychiatry. 2007; 68:e30. [PubMed: 18162010]

6. Chamberlain SR, et al. Orbitofrontal dysfunction in patients with obsessive-compulsive disorder and their unaffected relatives. Science. 2008; 321:421. [PubMed: 18635808]

7. Milad MR, Rauch SL. Obsessive-compulsive disorder: Beyond segregated cortico-striatal pathways. Trends Cogn. Sci. 2012; 16:43. [PubMed: 22138231]

8. Eagle DM, Baunez C. Is there an inhibitory-response-control system in the rat? Evidence from anatomical and pharmacological studies of behavioral inhibition. Neurosci. Biobehav. Rev. 2010; 34:50. [PubMed: 19615404]

9. Mar AC, Walker AL, Theobald DE, Eagle DM, Robbins TW. Dissociable effects of lesions to orbitofrontal cortex subregions on impulsive choice in the rat. J. Neurosci. 2011; 31:6398. [PubMed: 21525280]

10. Graybiel AM, Rauch SL. Toward a neurobiology of obsessive-compulsive disorder. Neuron. 2000; 28:343. [PubMed: 11144344]

11. Chen M, et al. Sapap3 deletion anomalously activates short-term endocannabinoid-mediated synaptic plasticity. J. Neurosci. 2011; 31:9563. [PubMed: 21715621]

12. Welch JM, et al. Cortico-striatal synaptic defects and OCD-like behaviours in Sapap3-mutant mice. Nature. 2007; 448:894. [PubMed: 17713528]

13. Zuchner S, et al. Multiple rare SAPAP3 missense variants in trichotillomania and OCD. Mol. Psychiatry. 2009; 14:6. [PubMed: 19096451]

14. Materials and methods are available as supplementary material on *Science* Online.

15. Morein-Zamir S, Fineberg NA, Robbins TW, Sahakian BJ. Inhibition of thoughts and actions in obsessive-compulsive disorder: Extending the endophenotype? Psychol. Med. 2010; 40:263. [PubMed: 19573261]

16. Steinmetz JE, Tracy JA, Green JT. Classical eyeblink conditioning: Clinical models and applications. Integr. Physiol. Behav. Sci. 2001; 36:220. [PubMed: 11777017]

17. Gage GJ, Stoetzner CR, Wiltschko AB, Berke JD. Selective activation of striatal fast-spiking interneurons during choice execution. Neuron. 2010; 67:466–479. [PubMed: 20696383]

18. Zhang F, Wang LP, Boyden ES, Deisseroth K. Channelrhodopsin-2 and optical control of excitable cells. Nat. Methods. 2006; 3:785. [PubMed: 16990810]

19. Mallet N, Le Moine C, Charpier S, Gonon F. Feedforward inhibition of projection neurons by fast-spiking GABA interneurons in the rat striatum in vivo. J. Neurosci. 2005; 25:3857. [PubMed: 15829638]

20. Kalanithi PS, et al. Altered parvalbumin-positive neuron distribution in basal ganglia of individuals with Tourette syndrome. Proc. Natl. Acad. Sci. U. S. A. 2005; 102:13307. [PubMed: 16131542]

21. Gittis AH, Kreitzer AC. Striatal microcircuitry and movement disorders. Trends Neurosci. 2012; 35:557. [PubMed: 22858522]

22. Crittenden JR, Graybiel AM. Basal ganglia disorders associated with imbalances in the striatal striosome and matrix compartments. Front. Neuroanat. 2011; 5:59. [PubMed: 21941467]

23. Canales JJ, Graybiel AM. A measure of striatal function predicts motor stereotypy. Nat. Neurosci. 2000; 3:377. [PubMed: 10725928]

24. Saka E, Goodrich C, Harlan P, Madras BK, Graybiel AM. Repetitive behaviors in monkeys are linked to specific striatal activation patterns. J. Neurosci. 2004; 24:7557. [PubMed: 15329403]

25. Eagle DM, et al. Contrasting roles for dopamine D1 and D2 receptor subtypes in the dorsomedial striatum but not the nucleus accumbens core during behavioral inhibition in the stop-signal task in rats. J. Neurosci. 2011; 31:7349. [PubMed: 21593319]

26. Kubota Y, et al. Stable encoding of task structure coexists with flexible coding of task events in sensorimotor striatum. J. Neurophysiol. 2009; 102:2142. [PubMed: 19625536]

27. Lee JH, et al. Global and local fMRI signals driven by neurons defined optogenetically by type and wiring. Nature. 2010; 465:788. [PubMed: 20473285]

28. Tye KM, et al. Amygdala circuitry mediating reversible and bidirectional control of anxiety. Nature. 2011; 471:358. [PubMed: 21389985]

29. Fentress, JC. The Biology of behavior. Kiger, K., editor. Corvallis, OR: Oregon State University; 1972. p. 83-132.

30. Aldridge JW, Berridge KC. Coding of serial order by neostriatal neurons: A "natural action" approach to movement sequence. J. Neurosci. 1998; 18:2777. [PubMed: 9502834]

31. Wan Y, Feng G, Calakos N. Sapap3 deletion causes mGluR5-dependent silencing of AMPAR synapses. J. Neurosci. 2011; 31:16685. [PubMed: 22090495]

32. Wan, et al. Circuit-selective striatal synaptic dysfunction in the Sapap3 knockout mouse model of obsessive-compulsive disorder. Biol. Psychiatry. 2013 Feb 13. [Epub ahead of print].
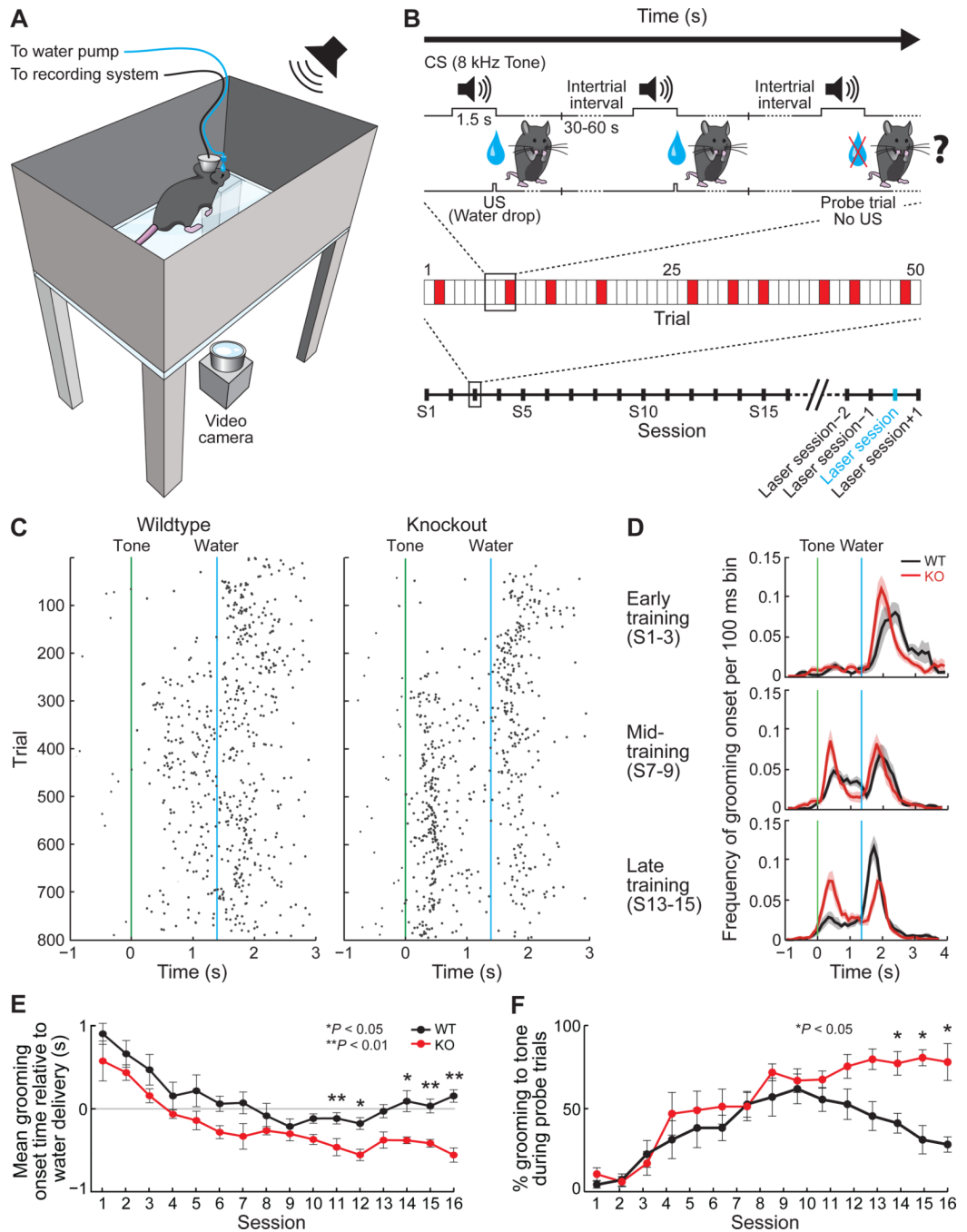
Fig. 1. *Sapap3* **mutant mice exhibit a deficit in adaptive grooming response during conditioning task**

(**A**) Grooming chamber. (**B**) Timelines. (Top) Three successive trials (two standard, one probe). (Middle) Session with 40 normal trials (white) and 10 randomly inserted probe trials (red). (Bottom) Full experiment (14). (**C**) Raster plots of grooming onsets (800 normal trials, 16 sessions), one mouse of each genotype. (**D**) Grooming onset distribution in wildtypes (WT) ($n = 5$) and knockout mutants (KO) ($n = 5$) in early, middle, and late training phases. Shading, SEM. (**E**) Mean grooming onset times [$n = 5$ mice/genotype; y axis zero, water drop; genotype effect, $P < 0.05$, repeated measures analysis of variance (ANOVA)]. (**F**)

Grooming to tone, probe trials (day-genotype interaction, $P < 0.01$, repeated measures ANOVA). (E) and (F) Error bars show SEM.
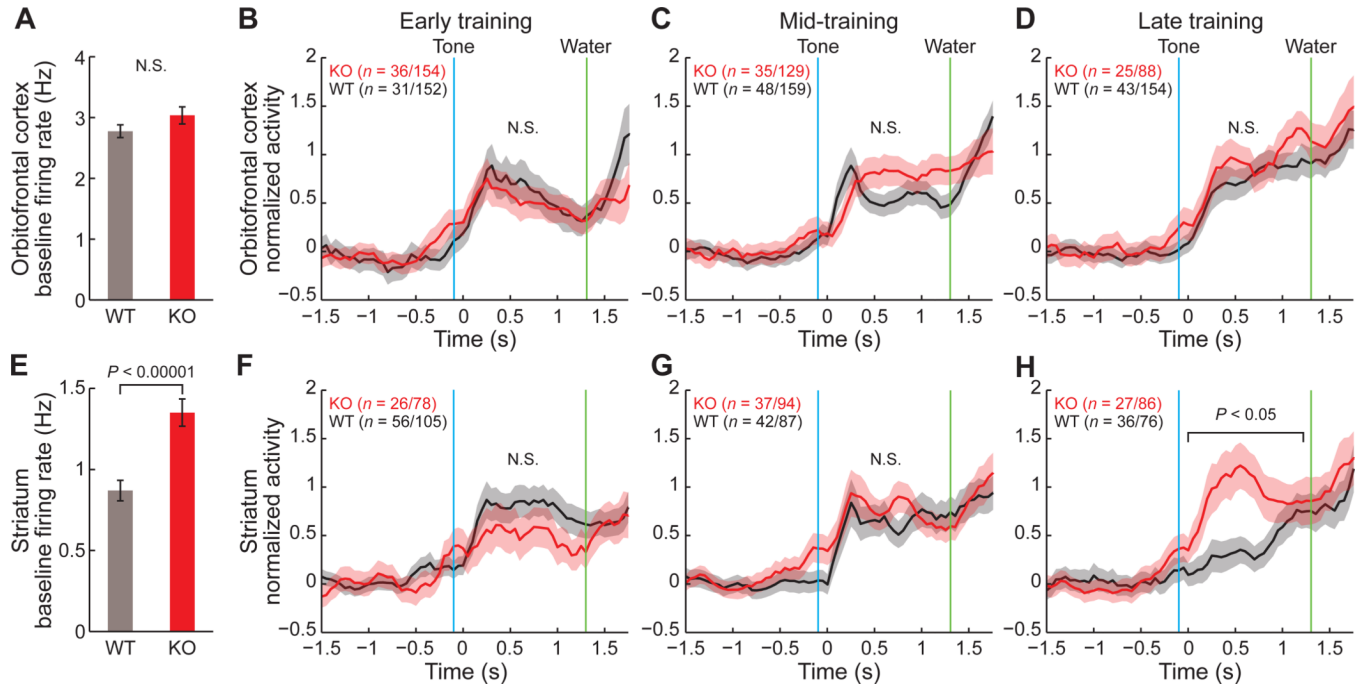
Fig. 2. Dynamic learning-related changes in lOFC and striatal ensemble activity differ in wildtype and *Sapap3* mutant mice

Average baseline firing rates of lOFC (**A**) and striatal (**E**) units. Average activity of lOFC (**B** to **D**) and striatal (**F** to **H**) units classified as task-responsive (i.e., firing preferentially between tone and water events relative to baseline activity). Mean z-scores normalized for each neuron relative to baseline activity for wildtype (WT) (*n* = 7) and *Sapap3* mutant (KO) (*n* = 7) mice during training. Above, ratios of task-responsive units to total units per genotype. Shading, SEM.
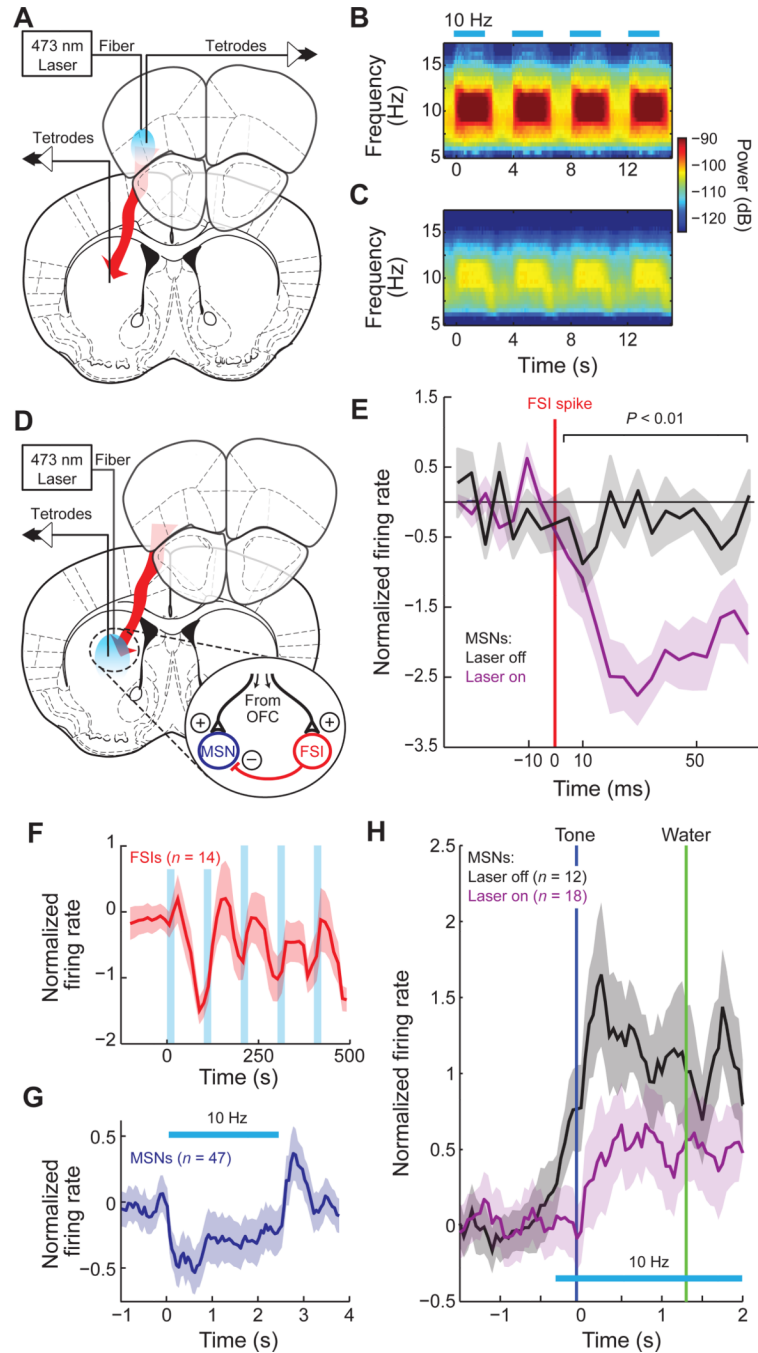
Fig. 3. Optogenetic stimulation of lOFC in *Sapap3* mutants enhances feed-forward inhibition in striatal circuitry
Simultaneous chronic recording and optogenetic stimulation in lOFC (**A**) and striatum (**D**) of mutants. LFP activity in lOFC (**B**) and striatum (**C**) at lOFC stimulation frequency (10 Hz, 5 mW, 5-ms pulse for 2.5 s, blue bars). (**E**) MSN spiking relative to FSI spikes (red line) during 2.5-s stimulation (purple) or no stimulation (black) of lOFC terminals in striatum (*n* = 10 FSI-MSN pairs recorded on the same tetrode, three mutants; stimulation effect *P* < 0.01, unpaired *t* test). Light stimulation (blue bars) induces synchrony of FSI population firing at stimulation frequency (**F**) (*n* = 14 units, three mutants) and long-lasting inhibition of MSNs during stimulation (**G**) (*n* = 47 units, three mutants). (**H**) Same stimulation

protocol applied at the end of the training significantly decreased MSNs firing (purple) relative to no-stimulation condition (black). Shading, SEM.
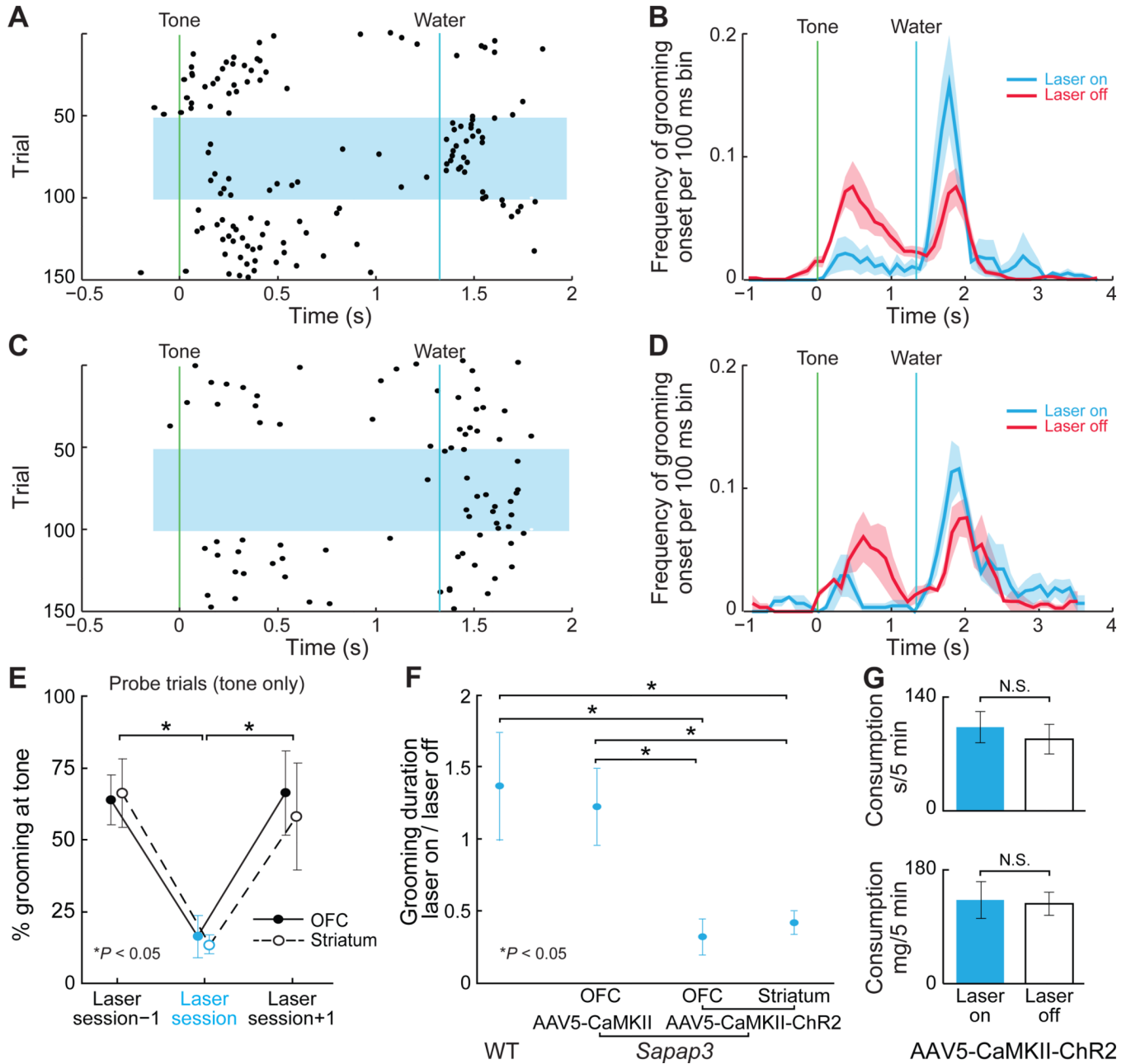
Fig. 4. Optogenetic stimulation of lOFC alleviates compulsive grooming of *Sapap3* mutant mice
Rasters of grooming onsets before, during (blue shading), and after bilateral lOFC (**A**) or
striatal (**C**) stimulation (10 Hz, 5 mW, 5-ms light pulses) in a *Sapap3* mutant, late in
training. Grooming onsets for the *Sapap3* population during session with laser stimulation
(blue) in lOFC (**B**) ($n = 4$) or striatum (**D**) ($n = 3$) compared with preceding laser-off session
(red). Shading, SEM. (**E**) Suppression of tone-evoked grooming by lOFC or striatal
stimulation during probe trials ($P < 0.01$, unpaired *t* test). (**F**) Alleviation of compulsive
grooming in *Sapap3* mutants ($n = 4$) by lOFC or striatal stimulation (5 Hz, 5 mW, 5-ms light
pulses) during 3-min free-movement periods, and control virus ($n = 3$) and wildtype ($n = 3$)
comparisons ($P < 0.05$, unpaired *t* test). (**G**) Lack of effect of same out-of-task lOFC

stimulation in mutants ($n = 4$) on time spent eating (top) or food consumed (bottom) during 5-min free-feeding periods. Error bars in (E to G), SEM.